A Broadband Phase and Power Control in RF Power Stations Based on Injection-locked Magnetrons*

G. Kazakevich[#], Muons, Inc., Batavia, IL, USA,
V. Lebedev, V. Yakovlev, Fermilab, Batavia, IL, USA,
V. Pavlov, Budker Institute of Nuclear Physics, Novosibirsk, Russia.

Capabilities of broadband phase and power control in injection-locked magnetrons were studied with a CW 2.45 GHz, 1 kW microwave oven magnetron. The study was aimed at the investigation of possible application of magnetrons for powering Superconducting RF (SRF) cavities in intensity-frontier accelerators. The study demonstrated that the magnetron RF phase can be controlled by injection of signal at power levels as low as about -12 dB in a frequency band of a few MHz with low phase and amplitude noise. Experiments verified that combining power of two injection-locked magnetrons with 3-dB hybrid yields a broadband phase and amplitude control in SRF cavity fed by the magnetron power station. The paper also discusses a simple theoretical model based on a kinetic approach which considers phase focusing in magnetrons and substantiates the experimental results.

PACS: 29.20.Ej, 84.40.Fe, 84.70.+p

Keywords: Magnetron, Injection locking, Transfer function characteristic, Transient process, Synchronous wave

Introduction

Power amplifiers feeding superconducting cavities in modern accelerators require a broadband phase and power control for suppression of parasitic modulations (microphonics, Lorentz Force Detuning (LFD), etc,) inherent to superconducting RF (SRF) cavities operation. Depending on the SRF cavity type and mode of operation the microphonics and LFD spectrum may extend from tens of Hz to about 1 kHz [1, 2]. Traditionally, linear RF amplifiers such as klystrons and IOTs are used in such high-power transmitters. They provide power up to hundreds of kW in CW mode at a carrier frequency in the GHz range with a bandwidth in the MHz range allowing compensation of the modulation. However, the unit cost of power for the traditional RF sources is quite high, ~ $5 per Watt and ~ $10 per Watt for the RF sources based on klystrons and IOTs, respectively [3, 4]. The cost of a unit of power of a commercial, L-band, CW high-power magnetron RF source is ≈$1 per Watt [4]. Since the magnetron has the highest efficiency compared to traditional RF amplifiers, the magnetron transmitters are attractive for RF sources in superconducting accelerators.

Injection-locked magnetrons were suggested in order to power linear accelerators [5]. Such proposal could work for normal conducting linac. However, it cannot be used in superconducting accelerators which require both RF phase and power control to suppress the parasitic modulations inherent to operation of SRF cavities.

* Work was supported by the US DOE grant DE-SC0006261 and collaboration Muons, Inc. - Fermilab
[#]e-mail: gkazakevitch@yahoo.com

Recently, two methods were suggested on how the power and phase of magnetron based transmitter can be changed with rates required for powering SRF cavities. The first one is based on combining signals of two phase-controlled magnetrons. Their signals are combined by the 3-dB hybrid and power control is achieved by the paraphasing of the signals [6]. The second method is based on the phase modulation of the signal locking a single magnetron [7]. Such modulation results in the power being distributed between the fundamental frequency and the sidebands. If the frequency of modulation is much higher than the cavity bandwidth the power concentrated in sidebands is reflected from the cavity. Thus, changes of the modulation depth result in the power change at the fundamental frequency.

Both methods use a large bandwidth of RF phase response of the injection-locked magnetrons clearly demonstrated in the experiments presented in Ref. [6]. We also would like to note that an implementation of phase and power control in SRF cavity would not be possible without modern FPGA (Field Programmable Gate Array) based digital feedback systems which were not readily available tens of years ago when the magnetrons were ruled out as a valuable power source for large-scale accelerators.

This paper presents an experimental study of the injection-locked magnetrons operating in the pulsed and CW regimes. The presented analysis of kinetics of drifting charge in the injection-locked magnetrons substantiates an increase of the magnetron stability, a decrease of the magnetron noise, and an increase of locking bandwidth with an increase of locking signal magnitude. The latter is related to an improvement of the azimuthal focusing of

charge by synchronous wave in the magnetron interaction space.

Methods of control of injection-locked magnetrons

A small power reflection from modern ferrite circulators allows us to consider an operation of the injection-locked magnetron decoupled from the load even in the case when the load reflects major fraction of the incoming power. In this case one can neglect the frequency (phase) pulling in the magnetron since the locking signal significantly exceeds the amplitude of the reflected wave.

It was experimentally verified that slow (relative to the magnetron oscillations) frequency/phase variation of the locking signal results in corresponding variation of the magnetron RF wave [8]. The slow variation can be considered as a transient process described by the abridged equation considering frequency/phase pulling and pushing in the injection-locked magnetron [9]:

$$\left\{\frac{d}{dt}+\frac{\omega_{0M}}{2Q_{LM}}\left(1-i\varepsilon_M\right)\right\}\widetilde{V}_M=\frac{\omega_{0M}}{Q_{EM}}\widetilde{V}_{FM}-\frac{\omega_{0M}}{2Q_{EM}Y_{0M}}\widetilde{I}_M. \quad (1)$$

Here Q_{LM}, and Q_{EM} are the magnetron loaded and external Q-factors, respectively, ω_{0M} is the frequency of the operating mode of magnetron cavity (typically π-mode), ω is the frequency (time-dependent in a general case) of the injection-locking signal, $\widetilde{V}_M$ and $\widetilde{V}_{FM}$ are phasors describing amplitudes of the oscillation in the magnetron cavity and in the injection-locking wave, respectively, $\widetilde{I}_M$ is the phasor of the first harmonic magnetron current, $\varepsilon_M=\tan\psi\approx 2Q_{LM}\left(\omega_{0M}-\omega\right)/\omega_{0M}$ is the detuning parameter, ψ is the angle between the sum of the phasors $\widetilde{V}_{FM}$ and $\widetilde{I}_M$ (taken with respective coefficients as shown in Fig. 1) and the phasor $\widetilde{V}_M$, $Y_{0M}=2\beta/R_{ShM}$ [1/Ohm] is the external waveguide conductance of the magnetron cavity, β is the magnetron cavity coupling coefficient, and R_{ShM} is the magnetron cavity shunt impedance. The Eq. (1) was derived using the Slowly Varying Envelope Approximation (SVEA) method [10]. The terms $\omega_{0M}\cdot\widetilde{V}_{FM}/Q_{EM}$ and $\omega_{0M}\cdot\widetilde{I}_M/(2Q_{EM}\cdot Y_{0M})$ are related to the modulation of the injection-locking signal and the modulation of the magnetron current, respectively. The latter results in phase pushing.

In a steady-state Eq. (1) is transformed into the following equation [10]:

$$\widetilde{V}_M=\cos\psi\cdot e^{i\psi}\left(\frac{2Q_{LM}}{Q_{EM}}\cdot\widetilde{V}_{FM}-\frac{Q_{LM}}{Q_{EM}\cdot Y_{0M}}\cdot\widetilde{I}_M\right). \quad (2)$$

The phasor diagram corresponding to Eq. (2) is shown in Fig. 1. As it is seen from the diagram a variation of the phase of the injection-locking signal or/and variation of the magnetron current cause a rotation of the magnetron voltage phasor, $\widetilde{V}_M$ [6].

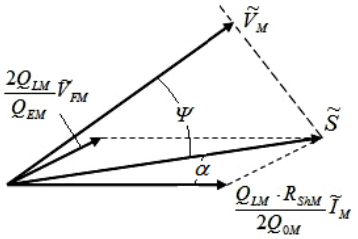

Fig. 1: Phasor diagram of the injection-locked magnetron in a steady-state, $Q_{0M}=\beta\cdot Q_{EM}$.

For the injection-locked magnetron in a steady-state the detuning parameter is constant. In this case the magnetron phase is bound to the phase of the locking signal. Fig. 1 demonstrates an effect of power of the injection-locking signal on rotation of the phasor $\widetilde{S}$. As one can see a variation of the magnetron current results in a change of its phase (phase pushing.) One can estimate the angle of rotation of the phasor $\widetilde{S}$ as:

$$\delta\alpha\cong\arctan\frac{4\beta\left|\tilde{V}_{FM}\right|}{R_{ShM}\left|\tilde{I}_M\right|}-\arctan\frac{4\beta\left|\tilde{V}_{FM}\right|}{R_{ShM}\left|\tilde{I}_M+\delta\tilde{I}_M\right|}.$$

As an example we consider 1 kW 2.45 GHz magnetron with β=10, $|\widetilde{V}_M|$= 2 kV, $|\widetilde{I}_M|$=0.4 A. Fig. 2 presents a dependence of ripple of the phasor phase $\widetilde{S}$ on the injection-locking signal for given magnetron current ripple. As one can see the phase variation is reduced with an increase of the locking signal. In the absence of other perturbations the angle Ψ does not change. Consequently, the phase variations of phasor $\widetilde{S}$ will be directly transferred to the phase ripple of magnetron RF voltage.

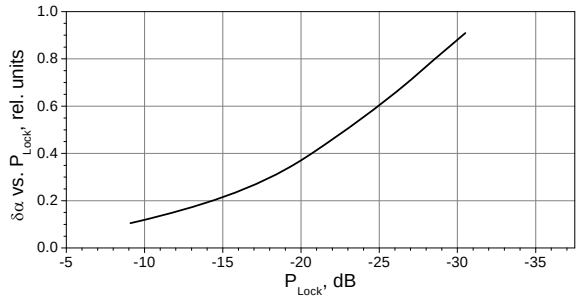

Fig. 2. Rotation of the phasor $\widetilde{S}$ indicating the phase pushing in a 2.45 GHz, 1 kW, CW magnetron model vs. power of the injection-locking signal.

A variation of the magnetron magnetic field also causes a rotation of phasor $\widetilde{V}_M$ relative to the phase of locking signal. The angle of rotation is also decreased with increase of the injection-locking signal [6]. Note also that different parameters have different spectra of their variations. The final spectrum of the magnetron phase variations is summed from the spectra of parameters variations.

Now, utilising a kinetic approach, we consider a conventional *N*-cavities magnetron with the magnetic field, *H,* above critical field. The magnetron is fed by a voltage somewhat below critical. The motion of electrons in the crossed magnetic and potential electric fields in the absence of generation may be described by a superposition of two circular motions: rotation of the electron at angular cyclotron velocity $\omega = eH/(mc)$ and motion of the centre of this circle around the coordinate frame centre at lower angular velocity Ω [14]. The latter motion represents a drift of the transported charge averaged over ω.

Taking into account axial symmetry the 2-D equations describing the motion of electrons in a magnetron are written in the polar coordinates [14, 15]:

$$\begin{cases} \ddot{r} - r\dot{\phi}^2 - \omega r\dot{\phi} = f_r \,, \\ r\ddot{\phi} + 2\dot{r}\dot{\phi} + \omega r = f_\phi \,. \end{cases}$$

Here $f_r = eE_r/m$, $f_\varphi = eE_\varphi/m$, $E_r = -U/\left[r\ln(r_2/r_1)\right]$, and U is the magnetron voltage. Thus the drift equations for the non-generating magnetron are [15]:

$$\begin{cases} \dot{r} = -\dfrac{c}{Hr}\dfrac{\partial \Phi^0}{\partial \phi} \cong 0 \,, \\ \dot{\phi} = \dfrac{c}{Hr}\dfrac{U}{\ln\left(r_2/r_1\right)r} = \dfrac{c}{Hr}\dfrac{\partial \Phi^0}{\partial r} \,. \end{cases} \tag{3}$$

Here Φ^0 is a potential of the static electric field, so that E_r=gradΦ^0, $\Phi^0 = \left[U\cdot\ln(r/r_1)\right]/\ln(r_2/r_1)$, $E_\phi(r) \simeq 0$, and the magnetron cathode and anode radii are denoted as r_1 and r_2.

Now we consider a magnetron operating in a steady-state being injection-locked by a small signal at the frequency, ω, which is a harmonic of charge rotation in the magnetron, Ω, so that $\omega = n\Omega$, where $n = N/2$, and N is the number of cavities as it was noted above.

We present the rotating slow synchronous wave in magnetron in the following form $e^{-i(n\varphi+\omega t)}$. The wave with the electric field $\vec{E}$ may be determined by the electric Hertz vector $\vec{\Pi}$ [16], so that $\vec{E} = grad\,(div\vec{\Pi}) + k^2\vec{\Pi}$ with the boundary condition $E_\varphi(r = r_1) = 0$, where $k=\omega/c$. The slow wave rotating in the interaction space of the magnetron with angular velocity $\Omega = -\omega/n$ can be presented by the potential $\Phi = -div\vec{\Pi}$ [16, 17] satisfying the equation for the vector $\vec{E}$:

$$\Phi = \frac{\tilde{E}_1\cdot r}{2n}\left[\left(\frac{r}{r_1}\right)^n - \left(\frac{r_1}{r}\right)^n\right]\sin\left(n\phi + \omega t\right) \,. \tag{4}$$

Here $\tilde{E}_1$ is amplitude of the radial RF electric field at $r = r_1$.

Then using the perturbation theory [14] we consider the motion of charge in the electric field with a potential $\Phi^0 + \Phi$. Then the equations of the charge drift in the generating magnetron are:

$$\begin{cases} \dot{r} = -\dfrac{c}{Hr}\dfrac{\partial}{\partial \phi}\left(\Phi^0 + \Phi\right), \\ \dot{\phi} = \dfrac{c}{Hr}\dfrac{\partial}{\partial r}\left(\Phi^0 + \Phi\right). \end{cases}$$

In coordinates rotating with the synchronous wave, assuming that $\varphi' = \varphi + \omega\cdot t/n$, one obtains:

$$\begin{cases} \dot{r} = -\dfrac{c}{Hr}\dfrac{\partial}{\partial \phi'}\Phi' \,, \\ \dot{\phi}' = \dfrac{c}{Hr}\dfrac{\partial}{\partial r}\Phi' \,. \end{cases}$$

where Φ' is an effective potential [15]:

$$\Phi' = U\frac{\ln(r/r_1)}{\ln(r_2/r_1)} + \frac{\omega H}{2nc}r^2 + \frac{\tilde{E}_1 r}{2n}\left[\left(\frac{r}{r_1}\right)^n - \left(\frac{r_1}{r}\right)^n\right]\sin(n\varphi') \,.$$

The first term determining azimuthal drift with linear velocity proportional to *1/r* is driven by radial distribution of the static electric field; the second one determines azimuthal drift with linear velocity *-(ω/n)r* in the synchronous wave frame; and the third term determines azimuthal and radial drifts caused by the RF electric field of the synchronous wave.

Let's rewriting Φ' in the following form:

$$\Phi' = \frac{U}{\ln\left(r_2/r_1\right)}\left[\phi_0(r) + \varepsilon\phi_1(r)\cdot\sin(n\varphi')\right],$$

where

$$\varepsilon = \tilde{E}_1/E_1 = \tilde{E}_1\cdot r_1\ln(r_2/r_1)/U \,,$$

$$\phi_0(r) = \ln\frac{r}{r_1} - \frac{1}{2}\left(\frac{r}{\breve{r}}\right)^2,$$

$$\phi_1(r) = \frac{1}{2n}\left[\left(\frac{r}{r_1}\right)^n - \left(\frac{r_1}{r}\right)^n\right],$$

$$\breve{r}^2 = -\frac{ncU}{\omega H\ln\left(r_2/r_1\right)} \,.$$

Then, one obtains the following drift equations describing charge motion in the operating magnetron [15]:

$$\begin{cases} \dot{r} = \omega\dfrac{\breve{r}^2}{r}\varepsilon\phi_1(r)\cos(n\varphi') \\ n\dot{\varphi}' = -\omega\dfrac{\breve{r}^2}{r}\left(\dfrac{d\phi_0}{dr} + \varepsilon\dfrac{d\phi_1}{dr}\sin(n\varphi')\right) \end{cases} \tag{5}$$

Here: $\breve{r}$ is a "synchronous radius" at which $d\phi_0/dr = 0$ (H<0 in the rotating frame) and the drift velocity of the charge is equal to the phase velocity of the RF wave.

The first equation in (5) represents the radial velocity of the drifting charge in the rotating frame. The second one represents the azimuthal velocity of the drifting charge related to the rotation of the frame and RF field. In accordance with the first equation, the drift of charge towards the anode is possible at $-\pi/2 < n\varphi' < \pi/2$ with a period of 2π, *i.e.* being focused in "spokes". The charge can enter the spoke through the boundaries located at $\pm\pi/2$.

The second equation describes the azimuthal velocity of the charge in the frame rotating with phase velocity of the synchronous wave. The first term in the brackets relates to an additional radially-dependent azimuthal drift of charge. It results in defocusing of the charge. Defocusing is absent at the "synchronous" radius, and the resonance focusing is quite efficient in forming "spokes" directed along the potential lines of the static electric field.

Analysis of Eqs. (5) shows that at low ε the stationary points appear where the radial and azimuthal velocities are zero. Consequently, the point locations are determined by following equations: $\dot{r} \cong 0$, $n\dot{\varphi}' = 0$. The solution results in that the points (see points A and B in Fig. 4) are located on boundaries of the azimuthal space allowed for a "spoke" *(-π/2, π/2)* and are determined by the equations: $n\varphi' = \pm\pi/2$, and $d\phi_0/dr = \pm d\phi_1/dr$. The coordinates of the stationary points are: *($r=r_A$, $n\varphi'=-\pi/2$)* for point *A*, and *($r=r_B$, $n\varphi'=\pi/2$)* for point *B*. The stationary points decrease the current of the magnetron and, in the worst case, may stop its operation. An increase of ε improves azimuthal focusing of charge and increases the velocity of radial drift stabilizing operation of the magnetron.

Fig. 3 presents a behaviour of the charge azimuthal velocity calculated at various ε for the simplified model with N=8 for a design considered in Ref. [15]. The calculation shows that the stationary points in the model disappear at $\varepsilon \geq 0.31$.

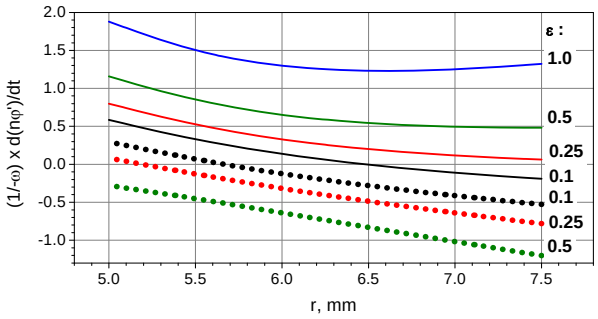

Fig. 3: Dependence of azimuthal velocity of charge on the radius in the space of interaction for various ε (shown on the right). The azimuthal velocity is in units $-\omega$; r_1 =5 mm, r_2 =7.5 mm, and $\bar{r}$ =6 mm. The solid and dotted lines are plotted for $n\phi' = \pm\pi/2$, respectively.

An increase of parameter ε, *e.g.* by an injection-locking signal with a sufficient magnitude, may significantly improve the focusing. It reduces a contribution of the defocusing term, $d\phi_0/dr$, to the charge motion towards the anode. Consequently, it makes the spoke more aligned with the radius as shown in Fig. 4. Better azimuthal focusing reduces the noise in the motion of spoke "centre of gravity" and, consequently, the magnetron noise [15].

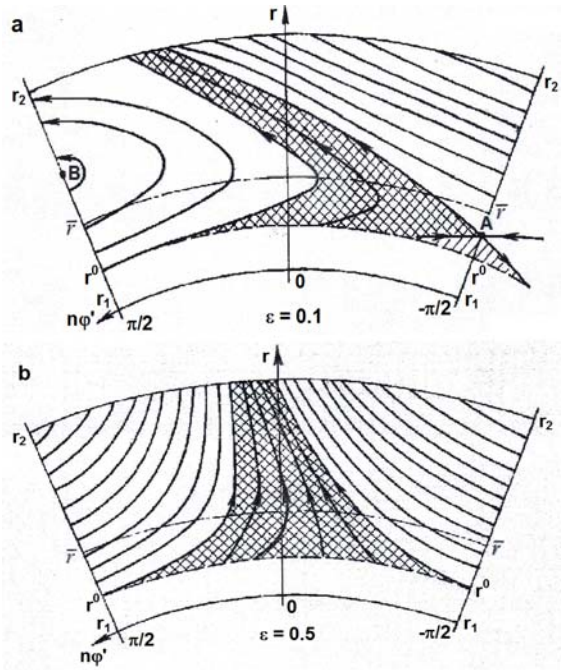

Fig. 4: Trajectories of the charge drift in "spokes" (shown by a crosshatching) at r^0/r_1 =1.1, r_2/r_1 =1.5, $\bar{r}/r_1$ =1.2; a) - ε=0.1, b) - ε =0.5 [15]. Radius r^0 shows position of the cathode layer. The arrows show drift of charge in "spokes" towards the magnetron anode

The injection-locking signal at a power level of -10 dB increases ε in the operating magnetron by ~30%. This notably improves the phase focusing of drifting charge for practically all radii of the drift trajectories in the magnetron space of interaction and decreases the phase noise.

The bandwidth of the phase control of the injection-locked magnetron is determined by quality factor of the magnetron cavity and duration of the transient process establishing the forced oscillation in the synchronous wave. An increase of ε increases radial velocity of the charge drift and improves the phase focusing. This widens the bandwidth of the phase control.

The discussed above kinetic approach was tested experimentally with injection-locked magnetrons operating in pulsed and CW regimes.

Experimental results

The influence of injection-locking signal magnitude on the bandwidth of the phase modulation was studied in experiments with 2.45 GHz, 1 kW, CW magnetrons operating in a pulsed regime with pulse duration of 5 ms. Experiments were performed with a single and a 2-cascade magnetrons injection-locked by the phase-modulated signal. The installation schematic is shown in Figs. 5 and 6 [11].

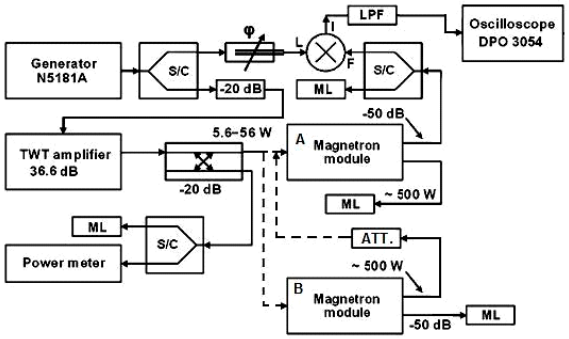

Fig. 5: Schematic of a single and 2-cascade (connections are shown by dashed lines) frequency-locked magnetrons at the phase modulation. S/C denotes splitter/combiner, LPF - low pass filter, ML - matched load, and ATT - attenuator. Details of modules A, B are shown in Fig. 6.

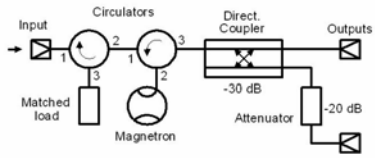

Fig. 6: Schematic of the magnetron module.

The single-cascade injection-locked magnetrons were tested in a configuration using only module *A*, as shown in Fig. 5. The magnetron was injection-locked by the CW TWT amplifier and operating in a pulsed regime with high voltage supplied by modulator. The module *B* was disconnected from the amplifier and the modulator.

The 2-cascade magnetron was tested in a configuration where the magnetron in module *B* was injection-locked by the TWT amplifier while the magnetron in module *A* was connected via attenuator to the module *B* output. Both magnetrons were powered by the same modulator. In this case the magnetron in module *A* was injection-locked by the signal of magnetron *B* reduced in the attenuator. Attenuation in the range of 13-20 dB [6, 11] did not affect the injection-locking.

Both single and 2-cascade injection-locked magnetrons were driven by N5181A generator. The generator signal was phase modulated by internal harmonic signal at frequency f_{PM}. Note that large bandwidth of TWT amplifier (2-4 GHz) resulted in no distortions of the phase-modulated signal injected to the first magnetron.

The bandwidth of phase response of the injection-lock was determined in two experiments. The first measurement used the Agilent MXA N9020A vector analyser in the regime of the phase modulation domain. The phase was modulated with magnitude of 4 deg. The analyser computed the magnitude of the phase modulation of the magnetron output. The results of the measurements averaged over 64 pulses for a number of frequencies in the frequency band from 30 kHz to 3 MHz are presented in Fig. 7 [6]. The reduction of phase response at high frequencies is mostly related to the magnetron bandwidth, $\Delta f \sim f_0 \cdot \sqrt{P_{Lock}} / 2Q \cdot \sqrt{P_{Out}}$, where f_0 is the magnetron frequency, P_{Out} and P_{Lock} are the power of magnetron and power of locking signal, respectively. The bandwidth of the magnetrons used in these experiments is in the range of few MHz depending on the magnitude of locking signal.

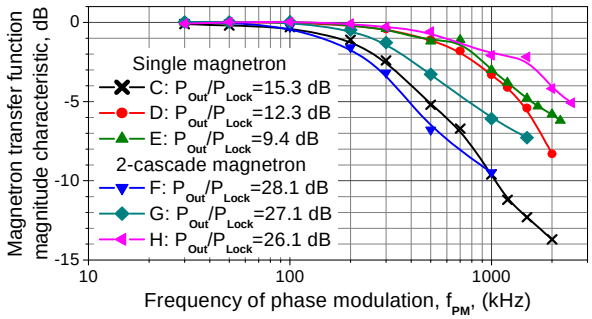

Fig. 7: Dependence of phase response magnitude on the frequency of phase modulation for the injection-locked magnetrons measured at various powers of the locking signal.

A phase detector, instead of vector analyser, was used in the second measurement. The phase modulated signal was split as shown in Fig. 5. One part of the signal was send to the magnetron and another was used as a reference for the phase detector. The magnitude of phase modulation was 20 deg. and the frequency of phase modulation was changed in the range of 10 kHz - 3 MHz [6]. Schematic of this experiment is shown in Figs. 5, 6. In this case the signal at the phase detector output bsuch measurement the

For simplicity the angle of the phasor rotation, θ was estimated approximately as: $\theta \approx \arccos(1 - V_O / V_{PM})$, or $\theta \approx \arcsin(V_O / V_{PM} - 1) + \pi/2$ at $V_O \leq V_{PM}$ and $V_O > V_{PM}$, respectively [6]. Here V_O is the voltage of the harmonic signal measured at the output of the phase detector. The phase detector voltage, V_{PM}, corresponding $\theta \approx 90$ deg. roughly considers instrumental function of the phase detector. The rotation of the phasor of voltage of the magnetron wave vs. frequency f_{PM} for various setups and powers of the phase-modulated injection-locking signal are plotted in Fig. 8.

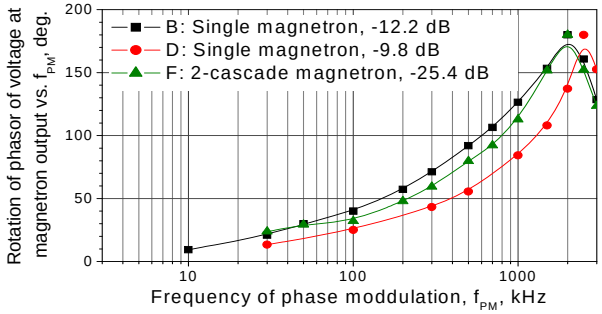

Fig. 8: Angles of rotation of the phasor of voltage in the wave at the output of the injection-locked magnetrons. The

angles were measured vs. the modulating frequency f_{PM} in various setups, at various locking powers.

The plotted phase characteristics of the magnetrons demonstrate that the available range of the phasor rotation is π (in reality ± π/2), It corresponds well to the phase area available for stable operation of the magnetron, Eqs. (5). In the range of this area all charge focused in "spokes" drifts towards the magnetron anode. An increase of the injection-locking signal *(ε)* improves the phase focusing widening the allowable bandwidth of the phase control, Fig. 8. Droop of the phase characteristics out of the phase range $\pm\pi/2$ results from loss of the non-focused charge.

The measured magnetron characteristics, Figs. 7, 8, are in good agreement. Fig. 8 verifies the developed kinetic approach for the magnetrons injection-locked by the phase-modulated signal.

The magnetron group delay, τ_g, plots vs. power of the injection-locking signal were computed from the measured phase characteristics. They are shown in Fig. 9 [11].

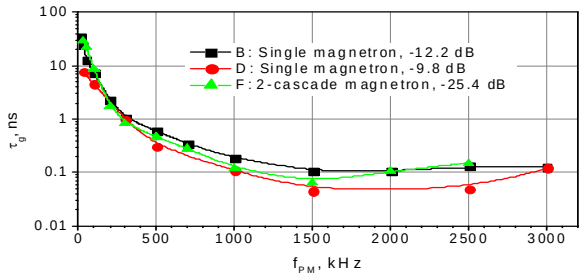

Fig. 9: The group delay, τ_g, obtained from the measured phase characteristics of the injection-locked magnetrons.

A decrease of the group delay at an increase of power of the injection-locking signal causes an improvement of the phase focusing. This indicates that the duration of the transient process of the phase modulation in the magnetron is reduced explaining the wider bandwidth of the phase control at the larger locking signal.

Decrease of the phase disturbances caused by variations of the magnetron current and the magnetron magnetic field by an increase of the locking signal in the injection-locked magnetrons was demonstrated in experiments in pulsed mode with the injection-locked single magnetron, Fig. 10.

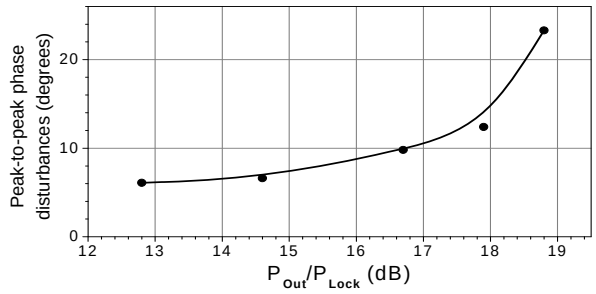

Fig. 10: Peak-to-peak phase disturbances of the injection-locked magnetron caused by phase pushing and perturbations of the magnetic field vs. power of the injection-locking signal, P_{Lock}, [6].

The plott in Fig. 10 shows that an increase of power of the injection-locking signal notably decreases the phase disturbances caused by phase pushing and perturbations of the magnetic field in the magnetron. The phase pushing was resulted from pulsed overheating of the magnetron cathode because of electron bombardment. Perturbations of the magnetron magnetic field were caused by the leakage field from the magnetron filament transformer and the filament circuitry. The plots in Figs. 2 and 10 demonstrate the same character of the magnetron phase response caused by the phase pushing or/and variation of the magnetic field on the locking signal value.

A simple scheme for deep and broadband power control was proposed and realized using a transmitter consisting of two injection-locked magnetrons (two-magnetron transmitter) which powers were combined by a 3-dB hybrid [6]. Power modulation was achieved by a regulation of the phase difference of two magnetrons by the analogue phase shifter JSPHS-2484 introduced into one of two channels (controlled channel), Fig. 10. The setup operated in pulsed mode with pulse duration is 5 ms.

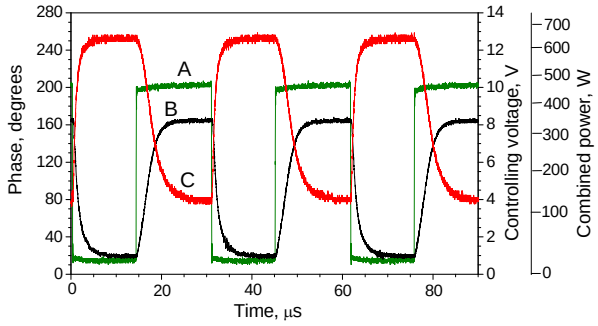

Fig. 10: Phase and power response of the two-magnetron transmitter to the phase difference of injection locking signals; trace A – the voltage controlling the phase shifter (the first scale on the right), Trace B – measured phase changes of the controlled magnetron (left scale), Trace C – output power of the transmitter (power measured at port "Σ" of the hybrid combiner, second scale on the right).

Effect of a phase modulation of the locking signal was studied measuring carrier frequency spectra of the 2.45 GHz, 1.2 kW magnetron in CW mode. The magnetron was fed by the switching power supply type SM445G. Fig. 12, [6], demonstrates measured precisely-stable carrier frequency at the broadband deep phase modulation.

Trace A shows the spectrum when the phase modulation is OFF; B- the phase-modulation is ON, f_{PM} =2 MHz and the magnitude is 3 radians; C is spectrum of the locking signal without the phase modulation.

The decrease of magnitude at the carrier frequency shown in the trace B is resulted from redistribution of power in carrier frequency spectrum and sidebands [6]. The

results substantiate method of power control proposed and realized in [7].

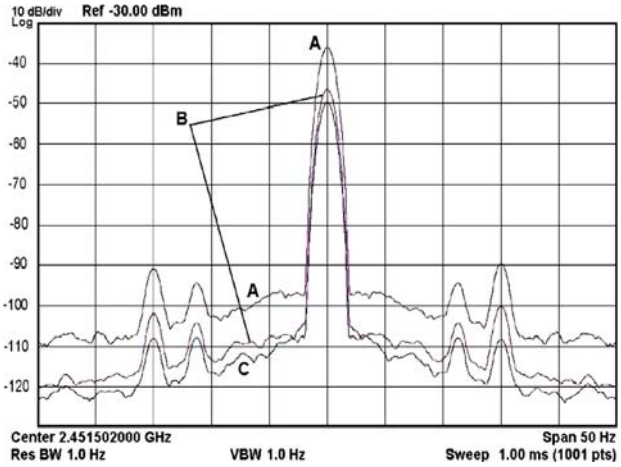

Fig. 12: Carrier frequency spectra of the injection-locked magnetron at P_{Out}/P_{Lock}= 13.4 dB, P_{Out}=850 W. vs. the broadband phase modulation. Scales in vertical and horizontal are: 10 dB/div and 5 Hz/div, respectively.

An increase of the injection-locking signal value, as it was noted above, reduces the magnetron noise, Fig. 13. The measurements were performed feeding the magnetron by switching power supply type SM445G. The magnetron was driven by a TWT amplifier fed by switch-mode power supplies. The sidebands caused by the TWT power supplies are clearly seen in the trace D showing spectral distribution of noise of the injection-locking signal.

The sidebands shown in the magnetron noise spectra result from the magnetron switching power supply and switching power supply of the TWT amplifier.

Plotted in Fig. 13, power densities in the sidebands caused by operation of the switch-mode power supplies of the magnetron are decreased with the increase of the injection-locking signal like effects of transient processes, as it was mentioned above. Note that at the sufficient injection-locking signal (P_{Lock}=100 W) power density in the sidebands caused by switching power supplies feeding the magnetron does not exceed -40 dBc/Hz.

Thus, operation of the injection-locked magnetrons at the relatively large power of the locking signal (-10 dB) allows broadband phase and power modulation (control) in magnetron low-noise transmitters. A CW transmitter with power combining based on 2-cascade magnetrons injection-locked by the phase modulated signal with power level up to -25 dB provides bandwidth of the phase, frequency and/or amplitude modulation in almost the same range as the less cost-effective and less efficient klystrons and IOTs.

The described experiments demonstrate that a large (up to –10 dB), phase-modulated injection-locking signal provides at a precisely-stable carrier frequency the widest bandwidth of control and higher stability to various transient processes.

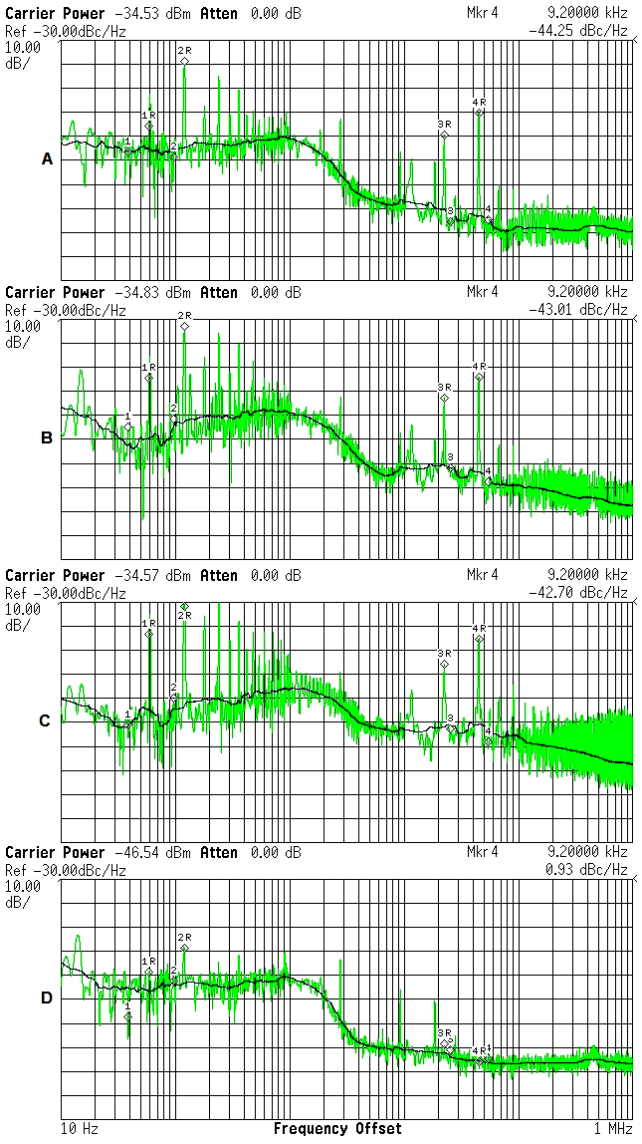

Fig. 13: Spectral distributions of noise of the CW injection-locked 2.45 GHz, 1.2 kW magnetron at the output power of 1 kW, vs. power of the locking signal of 100, 30 and 10 W, traces A, B and C, respectively. Trace D is spectrum of the injection-locking signal (P_{Lock}=100 W), the magnetron anode voltage is OFF. Black traces show averaged noise distributions.

Summary

The described experiments with 2.45 GHz commercial magnetrons injection-locked by a phase-modulated signal demonstrate the capability of the magnetrons for broadband (in the range of a few MHz) phase modulation at a precisely-stable carrier frequency, at a large (up to -10 dB per a magnetron in a 2-cascade device) power of the locking signal. The large locking signal notably decreases the magnitude of the phase noise and phase disturbances caused by various transient processes and widens the

bandwidth of the phase control. The presented kinetic approach substantiates application of a large injection-locking signal for broadband phase and amplitude modulation (control) of magnetrons at low phase noise. The measured magnetron characteristics verify correctness of the developed kinetic approach for the magnetrons injection-locked by a phase-modulated signal.

The Proof-of-Principle of broadband phase and power modulation (control) in the transmitter with power combining, based on magnetrons injection-locked by a relatively large phase-modulated signal has been demonstrated in experiments, [6]. The transmitter is suitable for any load impedance. The high-power transmitters providing precisely-stable carrier frequency are suitable for feeding the SRF cavities of intensity-frontier particle accelerators.

Injection-locking of magnetrons by a phase-modulated large signal provides the widest bandwidth of the phase and power modulation (control) allowing precise stabilization of the accelerating field in SRF cavities at high stability of the tubes.

Acknowledgements

We are very thankful to Dr. H. Edwards for her interest and permanent support of this work, to B. Chase and R. Pasquinelli for support and help in experiments and Drs. R. Thurman-Keup and W. Shappert for fruitful discussions.

References

[1] Z. Zheng, S. Zhao, Z. Liu, D. Morris, J. Wei, Y Zhang, "Study of microphonics compensation for SRF cavity", Proceed. of PAC2013, 1355-1357, 2013.

[2] W. Shappert, Y. Pischalnikov, "Resonance control in SRF cavities at FNAL", Proceed. of PAC2011, 2130-2132, 2013.

[3] R. Pasquinelli, "RF Power sources for Project X", https://indico.fnal.gov/contributionDisplay.py?sessionId=4&contribId=12&confId=6098.

[4] G. Kazakevich, "High-Power Magnetron RF Source for Intensity-Frontier Superconducting Linacs", EIC 2014, TUDF1132_TALK, http://appora.fnal.gov/pls/eic14/agenda.full

[5] T. Overett, D.B Remsen, E. Bowles, G.E. Thomas and R.E. Smith, "Phase locked magnetrons as accelerator RF sources",PAC 1987, Proceed., 1464-1465, Washington, DC, USA, 1987.

[6] G. Kazakevich, R. Johnson, G. Flanagan, F. Marhauser, V. Yakovlev, B. Chase, V. Lebedev, S. Nagaitsev, R. Pasquinelli, N. Solyak, K. Quinn, D. Wolff, V. Pavlov, Nuclear Instruments and Methods in Physics Research A 760 (2014) 19.

[7] B Chase, R. Pasquinelli, E. Cullerton, Ph. Varghese, JINST, 10, P03007, 2015.

[8] Grigory M. Kazakevich, Viatcheslav M. Pavlov, Young Uk Jeong, Byung Cheol Lee, Physical Review Special Topics—Accelerators and Beams 12 (2009) 040701.

[9] Grigory M. Kazakevich, Viatcheslav M. Pavlov, Young Uk Jeong, Byung Cheol Lee, Nuclear Instruments and Methods in Physics Research A 647 (2011) 10.

[10] Joint US-CERN-JAPAN international school on frontiers in accelerator technology, 9–18 Sept. 1996, World Scientific, ISBN 981-02-3838-X.

[11] G. Kazakevich, R. Johnson, B. Chase, R. Pasquinelli, V. Yakovlev, "Regime of a wideband phase-amplitude modulation in a CW magnetron transmitter with a phase control", http://arxiv.org/abs/1407.0304

[12] A.C. Dexter, G. Burt, R.G. Carter, and I. Tahir, H. Wang, K. Davis, and R. Rimmer, Physical Review Special Topics-Accelerators and Beams, 14, 032001, 2011.

[13] V. Lebedev, Limitation of current ripple of the power supplies for the SSC bending magnets, BUDKERINP 93-62 preprint

[14] P.L. Kapitza, HIGH POWER ELECTRONICS, Sov. Phys. Uspekhi, V 5, # 5, 777-826, 1963.

[15] L.A. Vanstein and V.A. Solntsev, in "Lectures on microwave electronics", Moscow, Sov. Radio, 1973.

[16] L.A. Vainstein, in "Electromagnetic waves", Moscow, Radio i Sviaz, 1988, ISBN 5-256-00064-0.

[17] D.I. Trubetskov and A.E. Khramov, Lectures on microwave electronics for physicists, V1, Moscow, Fizmatlit, 2003, ISBN 5-9221-0372-5.